Journal of Thermal Analysis and Calorimetry, Vol. 90 (2007) 3, 769–775

ZINC COATINGS FOR OXIDATION PROTECTION OF FERROUS SUBSTRATES
Part I. Macroscopic examination of the coating oxidation

G. Vourlias, N. Pistofidis, K. Chrissafis and G. Stergioudis*

Physics Department, Aristotle University of Thessaloniki, Thessaloniki 54124, Greece

The oxidation resistance of ferrous materials at elevated temperatures is limited. For that purpose the performance of zinc coatings deposited with hot-dip galvanizing, pack cementation and thermal spraying was considered. In the present work the oxidation resistance of these coatings at 400°C was estimated with light microscopy, thermogravimetric analysis and X-ray diffraction. From this examination it was deduced that in every coating a scale that was mainly composed of ZnO was formed, while Fe oxides were also detected in galvanized and pack coatings. However, the presence of the Fe/Zn phases inside the galvanized and pack coatings led to the formation of cracks, which could expose the substrate and thus destabilize the coating. This phenomenon was not observed in the thermal sprayed coatings, where the Fe/Zn phases were absent. In any case these cracks are not likely to jeopardize the resistance of the coating because zinc is anodic to steel. Hence, from the above examination it was deduced that the behavior of zinc coatings would be sufficient at 400°C.

Keywords: *coating materials, oxidation, thermal analysis, X-ray diffraction, zinc*

Introduction

Ferrous materials are widely used in different constructions due to their good mechanical properties, good formability and low cost. However they are prone to electrochemical corrosion and oxidation at high temperatures [1]. To overcome this disadvantage, different methods are used, among which the application of metallic and non-metallic coatings is one of the most common [2].

The oxidation of metallic materials at elevated temperatures is a well-studied phenomenon [1–6]. In this case, the oxidation mechanism postulates initial adsorption of oxygen on the clean metal surface, which forms a chemisorbed oxide layer. Additional layers of the oxide build up fast, usually via island growth. As oxidation advances, an observable oxide scale is formed.

The increase of the oxide layer is due to the fact that oxygen from the gaseous phase is reduced to oxygen ions at the scale/gas interface. The produced electrons from the oxidation reaction diffuse through the scale resulting to the formation of metal ions (cations) at the metal/scale interface. These cations along with the oxygen anions diffuse in opposite directions through the oxide layer and are combined to form metal oxide lattice sites. In regard to the conductivity of the two ionic species (metal cations and oxygen anions), the growth of the oxide layer could be at the metal/scale interface or at the scale/gas interface.

The formation of the oxide scale could inhibit the corrosion of the underlying metal [1–6]. This phenomenon is observed in the case of ferrous materials, where the growth of a layer composed by Fe oxides delays the degradation of the metallic substrate. However, the performance of iron or carbon steel under these conditions is not considered satisfactory. A possible solution to this problem is the application of adequate protective coatings. For temperatures up to 400°C, as in the case of piping installations for hot oils or superheated steam, organic or inorganic coatings are often used [7]. A common material for applications of this kind is zinc silicate, which is resistant up to 400°C [7]. However, the protective action of this coating is limited when the tubes are thermally insulated and as a result, moisture is accumulated at the coating/insulation interface when the piping system cools down. The presence of this film could destabilize zinc silicate. A more effective solution is the application of stainless steel tubes, which, although they are very efficient and resist moisture accumulation, are very expensive [8].

An alternative method that could be used instead is the application of metallic zinc coatings [9]. An overview of the deposition techniques of these coatings is presented in Table 1; while they are described with more details elsewhere [9, 10]. The usage of these coatings is compatible with the end-use of the

* Author for correspondence: hrisafis@physics.auth.gr

1388–6150/$20.00

Akadémiai Kiadó, Budapest, Hungary
Springer, Dordrecht, The Netherlands

Table 1 Major deposition techniques of metallic zinc coatings

Principle	Commercial method
Immersion in a molten zinc bath	hot dip galvanizing
Immersion in a chemical bath	electroplating
Spraying of molten zinc	thermal spraying (metallizing)
Chemical vapor deposition	pack cementation/fluidized bed reactor

coated pipes, because they could be applied only at the outer surface, as in the case of organic or other inorganic coatings. Extended and very accurate researches [10–23] indicate that they are very resistant to wet (aqueous) corrosion, as in the case of moisture accumulation underneath the insulation of piping systems that was previously mentioned. However, there is not any information about their performance at elevated temperatures, because of the low melting point of zinc (about 419°C [24]), which however does not prohibit its application at 400°C.

The aim of the present work is the examination of the behaviour of different zinc coatings at 400°C. For this reason the resistance of zinc at high temperature corrosion is initially examined by means of theoretical analysis, in order to estimate the feasibility of this project. In the experimental part, an effort is made to clarify the macroscopic behaviour of different zinc coatings (hot-dip galvanized, thermal sprayed and pack coatings) under the conditions in question. Electroplated coatings were excluded from this research due to their thickness, which is very low in regard to the other coatings [9]. This data is rather crucial because what really matters in industrial scale is the macroscopic behaviour. Consequently its description in details would be very useful.

In any case, this work is of great importance, if we take into account the total length of steam supplying networks in the chemical factories [25], which imposes the application of an inexpensive and effective anticorrosive coating. As a matter of fact, the failure of these networks due to oxidation is often responsible not only for delays in the production, but also for several accidents in the industry [26]. Therefore their anticorrosive protection is critical.

Preliminary assessment of zinc performance

As it was mentioned before, zinc is an ideal material for protection from electrochemical corrosion in aqueous environments [10–23]. However, its application at higher temperatures (below its melting point) could also be very beneficial, as the following analysis shows.

The oxidation durability of a metal could be roughly predicted with the application of the empirical criterion of Pilling–Bedworth (Pilling–Bedworth ratio [1–6]), which refers to the volume ratio of oxide and metal per gram-atom of metal and could be calculated by the following equation:

$$R = \frac{Md}{\alpha mD} \quad (1)$$

In this equation M and D refer to the molecular mass and the density of the metal oxide, m and d to the molecular mass and the density of the base metal and α to the stoichiometric factor of the metal in the oxide formula (M_aO_b). When the Pilling–Bedworth ratio is below 1 or much higher than 1, insufficient oxidation resistance is expected. Otherwise, the oxidation resistance is expected to be good. In the case of the system Zn/ZnO, the Pilling–Bedworth ratio equals to 1.627. Thus, ZnO could be protective to the underlying zinc. In this case only the formation of ZnO is supposed, because ZnO_2 (zinc hyperoxide) is decomposed at 212°C [24] and as a result the Zn scale at 400°C is seemingly composed only by ZnO.

However, the oxidation performance of a metal is also affected by other factors [1–6, 27]. More specifically, in order to obtain effective protection by the scale, certain properties are demanded by the oxide(s) formed. These properties are summarized in the following list:

- low vapour pressure of the scale at the operating temperature
- high melting point (above the operating temperature) of the scale
- low ionic flux through the scale

In the case of the Zn/ZnO system these factors are fulfilled. Concerning the first condition, as it could be predicted from the Ellingham diagrams [2], ZnO is stable up to 400°C, while it is neither evaporated nor decomposed. Nevertheless, its melting point is 1975°C [24], which is much greater than the operating temperature (400°C).

The ionic flux through the scale could be estimated by the diffusivity of zinc and oxygen in ZnO. Although this data is highly affected by the temperature and there are many estimations and models [28, 29], the diffusivity of zinc in ZnO is of the order of 10^{-6} cm^2 s^{-1} and the diffusivity of oxygen in ZnO is of the order of 10^{-15} cm^2 s^{-1}. Consequently, the ionic flux through the scale is rather low. For comparison reasons the diffusivity of oxygen in Fe_2O_3 is mentioned, which is reported to be about 10^{10} cm^2 s^{-1}, while the diffusivity of Fe in Fe_3O_4 is about 10 cm^2 s^{-1} [2].

From this information, it could be deduced that zinc is resistant at elevated temperatures. However, its low melting point limits the application tempera-

ture up to 419°C. After this temperature catastrophic oxidation is expected, since the zinc coating melts and collapsing is expected. However, it is very probable that zinc would offer satisfactory protection to ferrous substrates at 400°C.

Experimental

Materials

Commercial, hot-rolled low carbon steel sheets were used as substrates for the sample preparation. The steel designation was U St-34 (C≤0.17, Mn: 0.20–0.50, S≤0.05, P≤0.08). Rectangular coupons have been cut from the steel sheet with sizes ranging from 100 mm long×30 mm wide×3 mm thick to 5 mm long×3 mm wide×2 mm thick.

Methods

Coating methods

Hot-dip galvanizing took place in a Thermolyne 1400 electric furnace inside a graphite crucible. The dipping time was 3 min and the zinc temperature was 450±2°C. Prior to galvanizing, the coupons were degreased in a solution of a non-ionic tenside containing H_3PO_4, pickled (deoxidized) in an aqueous solution containing 16% HCl and fluxed in an aqueous solution containing 50% $ZnCl_2 \cdot 2NH_4Cl$. The average coating thickness of the hot-dip galvanized coatings, as it was determined metallographically, was about 80–100 μm.

Pack cementation was accomplished in porcelain crucibles, filled with powder mixture containing 2% NH_4Cl, 50% Zn and the rest Al_2O_3. The ferrous substrates were immersed in this mixture. The crucibles were covered with porcelain lids, sealed with high temperature resistant cement and placed in a tubular argon-purged electric furnace at 400°C for 60 min [19]. The average coating thickness for this method was close to the thickness of the hot-dip galvanized coatings (about 60–90 μm).

For the samples deposited with thermal spraying, a METCO 14E wire flame spray device was used. The distance between the flame and the substrate was 120 mm, the combustible gas was acetylene and the wire used had a 2.4 mm diameter and it was composed by 99.9% pure Zn. Prior to the coating deposition, the surface of the ferrous substrates was sandblasted. The thickness of the as-cast coatings was about 150–200 μm. The excessive thickness with regard to the methods mentioned before, is an inherent characteristic of thermal spraying.

Corrosion study

For the examination of the oxidation, the specimens were exposed in a laboratory electric furnace equipped with a ventilation system. The ventilation system ensured good air circulation, without affecting the atmospheric pressure in the furnace. The temperature of the furnace was settled at 400°C and the exposure time was 24 h. Samples of bare (uncoated) steel were also placed in the furnace for comparison reasons.

Instrumental methods

For the in situ study of the oxidation of the coatings thermogravimetric measurements were used. They were carried out with a Setaram SETSYS TG-DTA 1750°C. The samples were placed in alumina crucibles. An empty alumina crucible was used as reference. For the isothermal experiments, the samples, at first, were heated from ambient temperature to 400°C in a 50 mL min^{-1} flow of air, with heating rate of 10°C min^{-1}. The samples remained for 24 h at this temperature. For comparison reasons a coupon of bare steel was also examined under the same conditions.

Apart from the TG, the usage of the laboratory furnace was considered necessary, because its size allows the examination of larger samples. This fact has two advantages. First, the samples are suitable for examination with XRD as it will be explained later. Furthermore, the larger size of the samples offers more representative results, because it is closer to the scale of the objects used in real applications. On the other hand, TG offers the possibility to observe oxidation in situ, which is not possible with the laboratory furnace.

For the study of the degradation progress, the surface of the corroded specimens was examined with a Karl Zeiss M8 low magnification binocular light microscope equipped with a CCD camera for image capture.

The nature of the phases formed after corrosion was determined with X-ray diffraction (XRD). For these experiments a 2-cycle SEIFERT 3003 TT diffractometer (CuK_α radiation) with Bragg–Brentano geometry was used.

For comparison reasons, apart from the corroded specimens, the macroscopic appearance and the morphology of the non-corroded specimens were also examined with the equipment mentioned before, in order to have a better estimation of the corrosion progress. The examination of the non-corroded samples was accomplished with Scanning Electron Microscopy using a 20 kV JEOL 840 A SEM, equipped with an Oxford ISIS 300 EDS analyzer.

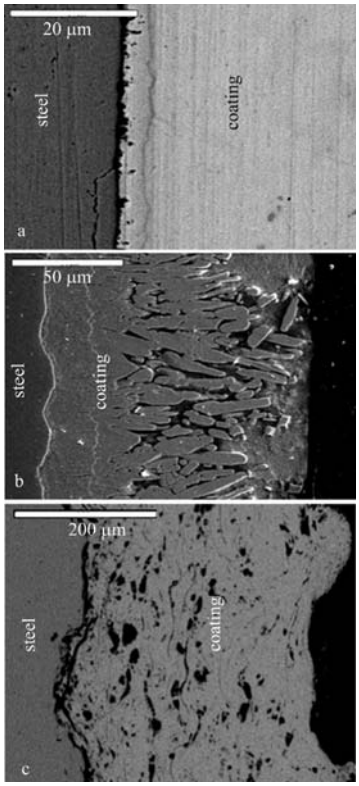

Fig. 1 SEM micrographs of the cross-section of a – a hot-dip galvanized, b – a pack and c – a thermal sprayed coating prior to corrosion

Results and discussion

Non-corroded samples

The macroscopic appearance and the morphology of the non-corroded zinc coatings are presented in Fig. 1. From these micrographs it is obvious that the surface of the galvanized and the pack coatings is rather smooth, characterized only by a little roughness. However, the surface of the thermal sprayed coatings is very rough. Deep cavities are observed with an average length of about 10–20 μm.

Furthermore, the morphology of the cross-section of the same coatings is the typical one. In the case of galvanized coatings, three layers are distinguished based on their relief. Their EDS microanalysis implies that they refer to δ, ζ and η phase of the Fe–Zn phase diagram. The pack coatings are composed by only two zones which correspond to Γ and δ phase of the Fe–Zn system. By contrast, in the case of the thermal sprayed coatings only a layer of pure zinc is identified, since diffusion does not take place.

The above mentioned phases are stable up to 400°C. Pure Zn is not melted at this temperature, while the Fe–Zn phases are characterized by much higher melting points [10]. Also, no metallurgical transformations are observed at such a low temperature in the galvanized coatings [10]. Hence the only phenomenon that takes place during heating of zinc coatings up to 400°C is superficial oxidation.

Corroded samples

In previous work [30] zinc thermal sprayed coatings were examined non-isothermally with TG. In this case it was deduced that mass increase begins at about 380°C. Up to this temperature the mass change is almost null. With the assistance of other experimental methods (SEM and XRD), it was verified that the mass increase is provoked by oxidation of the zinc surface, which leads to the formation of ZnO layer (scale). Furthermore it was observed that, above 419°C the oxidation rate increases due to the zinc melt which takes place at this temperature and results to the stripping of the ferrous substrate. Hence the most convenient temperature was considered to be 400°C, which is also more suitable for industrial applications [7]. The examination of hot-dip galvanized and pack coatings under the same conditions showed that these coatings also have the same behaviour. Consequently, a temperature of 400°C was chosen in the present work for all the isothermal experiments.

The oxidation was studied in-situ with thermogravimetric measurements. For that purpose the samples were isothermally heated at the selected temperature (400°C) for 24 h. This procedure led to an increase of the mass of each sample and it is summarized in the TG plots of Fig. 2. In these plots the mass change per surface unit as a function of time is presented. The fraction of the mass change to the area of the exposed surface was used because the oxidation of each material is affected by the exposed surface and not by its initial mass.

The relative position of these curves does not indicate only the different oxidation resistance, but it is also affected by another factor, which is the size of

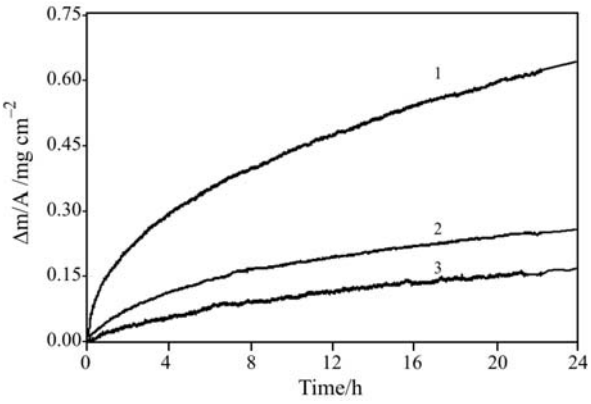

Fig. 2 Thermogravimetric plot of the mass change per unit of surface for the different coatings *vs*. time after about 24 h of exposure at 400°C; 1 – thermal spray coating, 2 – galvanized coating, 3 – pack cementation coating

the coating surface exposed in the hot air. Since TG offers only the mass change of each sample, measurements of the coating surface are necessary to draw the curves of Fig. 2. In our experiments the size of the corroded surface was supposed to be equal to the geometrical surface of each coating. The measurements of these surfaces were accomplished through length measurements of the examined coupons. However, these measurements include a certain error, even when they are realized in a microscopic scale. Especially in the case of thermal sprayed coatings, the true coating surface which was oxidized is much higher than the calculated one, due to its high roughness. As a result, the calculated value for the mass change per surface unit is higher than the real value which would be calculated if the exact coating surface was measurable. For this reason, the oxidation progress of the thermal sprayed coatings seems to be higher with regard to the others.

By contrast, in the case of the other coatings the curves are very close to each other. If we take into account the fact that macroscopical examination shows that the roughness of both these coatings is seemingly the same [10, 23], this observation is justified. However, this opinion has to be supported by precise surface measurements. This data would also allow the formulation of exact equations describing the oxidation kinetics. In any case in this work this analysis did not take place, because our main goal was the determination of the oxidation mechanism.

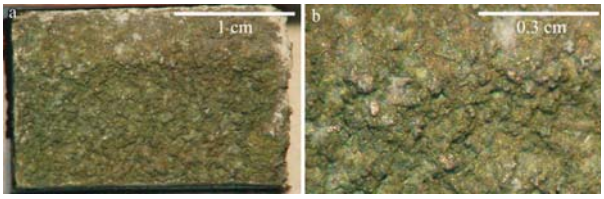

Fig. 3 Plain view photograph of the surface of zinc thermal sprayed coating after 24 h of exposure at 400°C; a and b – refer to different magnification

The scale formation, which was detected through the mass change of the samples exposed in the TG, was also visually observed. The changes of their appearance are obvious even with a naked eye (Figs 3–5). The typical silver-grayish color of the zinc coatings disappeared. Instead, a darker gray hue is observed, which is probably due to the formation of the oxide scale.

In the case of hot-dip galvanized coatings reddish-brown spots could also be distinguished (Fig. 4), while in the case of pack coatings this phenomenon is much more intense (Fig. 5). This coloration is likely to be attributed to the formation of iron oxides (red rust). However, it does not indicate failure of the coating and exposure of the substrate. Most probably it is

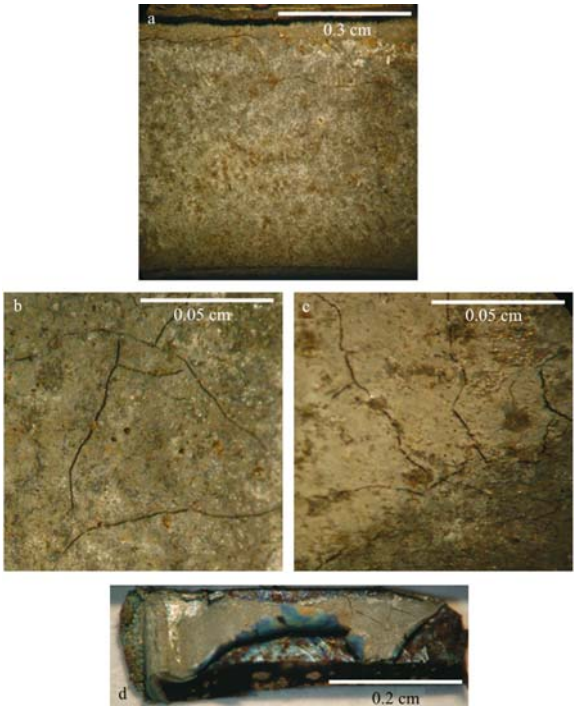

Fig. 4 Plain view photograph of the surface of a hot-dip galvanized coating after 24 h of exposure at 400°C; a, b and c – refer to different magnification, d – a galvanized sample is also presented. This sample was cut from a larger coupon prior to oxidation and afterwards exposed in the TG apparatus for 24 h

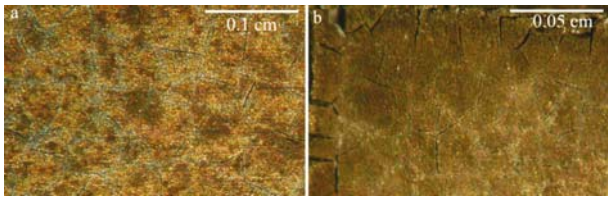

Fig. 5 Plain view photograph of the surface of a zinc pack coating after 24 h of exposure at 400°C; a and b – refer to different magnification, b – focused on the edge of the coupon

due to the Fe content of the coating which is also oxidized as it will be later presented with EDS. For the hot-dip galvanized samples this content is rather low [10] and as a result the extend of red spot formation is low. However, in the case of the pack coatings, the Fe content is much higher [17] and thus the Fe oxide formation is much more extensive.

What is rather characteristic in these photographs is the crack formation in the hot-dip galvanized and pack coatings. This phenomenon is more intense in the case of the pack coatings, where delamination of the coating at the edges of the sample is observed (Fig. 5b). By contrast, in the galvanized coatings (Figs 4a–c) the coating adhesion is not affected, but a dense crack network covers the coating surface.

This phenomenon could be attributed to the mismatch of the thermal expansion coefficients of zinc, Fe/Zn phases and Fe. As it is observed in Fig. 1 and explained in more details elsewhere [10], galvanized coatings are composed by four successive layers. Three of them, which are adjacent to steel, refer to Fe/Zn phases, while the fourth one, which is mainly composed by zinc, seals the system. Pack coatings have also a laminar structure although only two layers are present that correspond to Fe/Zn phases [16, 31]. The layer of zinc which covers galvanized coatings is absent in this case.

Each one of these phases is characterized by a different thermal expansion coefficient. The higher value is recorded for pure Zn, while Fe has the lowest [32]. The Fe–Zn phases are located in the intermediate and their values increase as their Zn content increases.

At elevated temperatures, as the samples are heated, both the substrate and the coating expand. However, the dimensional change of the substrate is not in accordance with that of the coating. As the coefficient of iron is the lowest of the system, the expansion of the substrate is much lower than the expansion of the coating. Hence compressive stresses are induced in the later, because, due to its adhesion to the substrate, it is not allowed to take the length referring to its coefficients.

In the case of galvanized and pack coatings, the high hardness and low ductility of Fe–Zn phases [32] result to the relief of these stresses through cracking. The phenomenon is more intense in the pack coatings, due to the absence of the outer phase (η phase). This phase is softer and more ductile because of the low iron content and as a result it could relief higher stresses prior to cracking and it prevents peeling.

In the case of zinc thermal sprayed coatings, the absence of cracks could be explained by the fact that the Fe–Zn phases are absent, since this coating is composed only by pure zinc [26, 33]. High ductility and low hardness of zinc result to a relief of the induced stresses through plastic deformation of the coating without cracking.

In Fig. 4d a galvanized sample is also presented. This sample was cut from a larger coupon prior to oxidation and afterwards exposed in the TG apparatus for 24 h. Its attack, as far as it concerns peeling, seems to be much more severe compared to the samples of Figs 4a–c. This phenomenon could be explained by the fact that cutting preceded oxidation. The internal stresses that this process introduced led to the extreme deformation of the coating. For this reason thermogravimetric analysis was accomplished with samples of adequate dimensions where machining was not necessary.

In any case, cracking and delamination are disadvantages for a coating, because they create paths

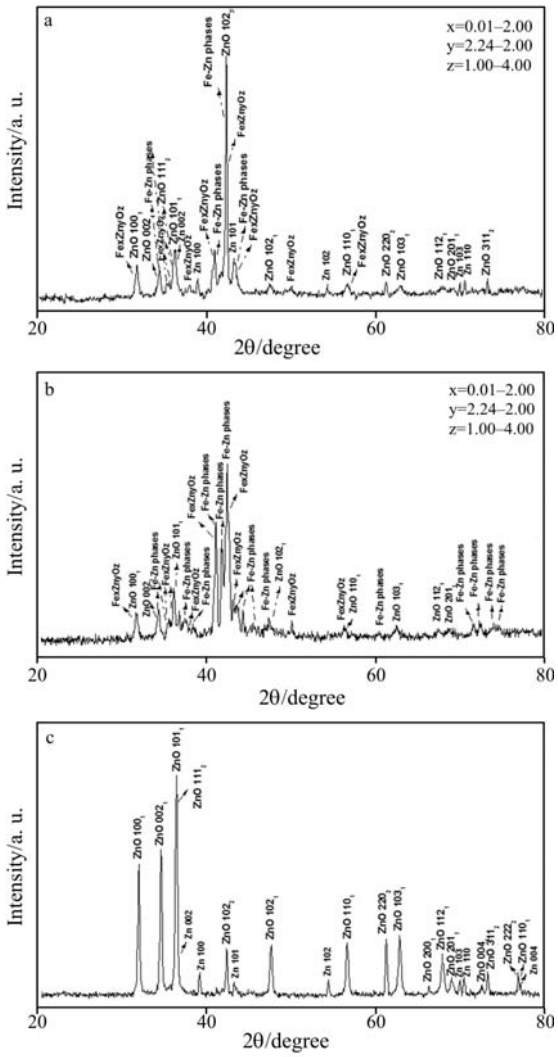

Fig. 6 XRD patterns of the oxidized coatings; a – galvanized, b – pack and c – thermal sprayed coating after 24 h of exposure at 400°C

which facilitate oxygen diffusion up to the ferrous substrate. However, since zinc is anodic with regard to iron, its protective action is not inhibited [11].

The composition of the scale on the corroded samples was verified with XRD (Fig. 6) (PDF#81-0683, PDF#81-0683, PDF#48-0567, PDF#34-1127, PDF#87-0713, PDF#77-0191, PDF#89-1397 [34]. So, in the case of galvanized and pack coatings, ZnO along with mixed Zn and Fe oxides were identified. Zn was also detected. The XRD pattern of the thermal sprayed coatings was a little different. The reflections recorded refer to ZnO and Zn for the thermal sprayed coating, while Fe oxides or mixed Zn–Fe oxides were not detected, because the coating does not contain any iron. This information is rather expected, since they were predicted during the theoretical analysis that took place initially. Apart from ZnO no other zinc oxides were detected. The existence of oxides with different stoichiometry is due

to the formation of mixed crystals of iron and zinc oxides when the coating is reach in iron. Hence it could be deduced that the scale is mainly composed by ZnO which offers the necessary protection.

Conclusions

Every zinc coating that was examined during the present work (galvanized, pack, thermal sprayed), when exposed in the air at 400°C is covered by a scale, which is primarily composed by ZnO. Iron oxides were also detected in the case of the galvanized and pack coatings. Both these oxides are expected to inhibit the zinc oxidation and consequently to protect the ferrous substrate.

However, in the case of galvanized and pack coatings a crack network was formed on their surface due to the mismatch of the thermal expansion coefficients of the coating and the substrate. This network offers paths to the oxygen ions. Thus, it seems that it facilitates oxidation. Nevertheless, the zinc protection even in the case of cracks is not inhibited, because zinc is anodic to steel [10].

As a result the macroscopic examination implies that zinc coatings are effective for oxidation protection up to 400°C. However, the formulation of solid conclusions and the exclusion of every doubt necessitate the microscopic examination of the same phenomena, which will also clarify the corrosion mechanism. Only under this condition long-term predictions would be accurate.

References

1 M. G. Fontana, Corrosion Engineering, 3rd Ed., McGraw-Hill, New York 1986.
2 I. G. Wright, ASM Handbook, Vol. 13 – Corrosion, ASM International, New York 1996.
3 J. R. Davis, Ed., Heat-Resistant Materials, ASM International, New York 1997.
4 F. J. Claus, Engineer's Guide to High Temperature Materials, Addison-Wesley Publishing Co., 1969.
5 G. Y. Lai, High Temperature Corrosion of Engineering Alloys, ASM International, New York 1990.
6 N. Birks and G. H. Meier, Introduction to High Temperature Oxidation of Metals, Edward Arnold, 1983.
7 M. J. Mitchell, Developments in Coatings for High Temperature Corrosion Protection, Proceedings of the Society of Protective Coatings 2002 Technical Presentations, Tampa, Florida, November 3–6, 2002, pp. 88–96.
8 J. R. Davis, Ed., Heat-Resistant Materials, ASM International, New York 1997.
9 Zinc coatings, American Galvanizing Association, Englewood, Colorado 2000.
10 A. R. Marder, Prog. Mater. Sci., 45 (2000) 191.
11 X. G. Zhang, Corrosion and Electrochemistry of Zinc, Plenum Press, New York 1996.
12 S. Oesch and M. Faller, Corros. Sci., 39 (1997) 1505.
13 V. Ligier, M. Wery, J. Y. Hihn, J. Faucheu and M. Tachez, Corros. Sci., 41 (1999) 1139.
14 A. R. Mendoza and F. Corvo, Corros. Sci., 42 (2000) 1123.
15 E. Almeida, M. Morcillo and B. Rosales, Brit. Corr. J., 35 (2000) 284.
16 E. Almeida, M. Morcillo and B. Rosales, Br. Corros. J., 35 (2000) 289.
17 G. Vourlias, N. Pistofidis, D. Chaliampalias, E. Pavlidou, P. Patsalas, G. Stergioudis, D. Tsipas and E. K. Polychroniadis, Surf. Coat. Technol., 200 (2006) 6594.
18 N. Pistofidis, G. Vourlias, E. Pavlidou, K. Chrissafis, G. Stergioudis, E. K. Polychroniadis and D. Tsipas, J. Therm. Anal. Cal., 84 (2006) 417.
19 N. Pistofidis, G. Vourlias, D. Chaliampalias, E. Pavlidou, K. Chrissafis, G. Stergioudis, E. K. Polychroniadis and D. Tsipas, J. Therm. Anal. Cal., 84 (2006) 191.
20 G. Vourlias, N. Pistofidis, G. Stergioudis and D. Tsipas, Cryst. Res. Technol., 39 (2004) 23.
21 G. Vourlias, N. Pistofidis, G. Stergioudis, E. Pavlidou and D. Tsipas, Phys. Status Solidi, A: Appl. Res., 201 (2004) 1518.
22 N. Pistofidis, G. Vourlias, D. Chaliampalias, E. Pavlidou, G. Stergioudis and E. K. Polychroniadis, Surf. Interface Anal., 38 (2006) 252.
23 G. Vourlias, N. Pistofidis, D. Chaliampalias, E. Pavlidou, G. Stergioudis, D. Tsipas and E. K. Polychroniadis, Corros. Eng. Sci. Technol., 41 (2007) in press (DOI: 10.1179/174327807x159899)..
24 CRC Handbook of Physics and Chemistry, 57th Ed., CRC Press, 1976–77.
25 D. Kern, Process Heat Transfer, McGraw-Hill, New York 1972.
26 J. M. Stellman, Ed., Encyclopedia of Occupational Health and Safety, 4th Ed., ILO, Geneva 1998.
27 S. Datta and S. Das, Bull. Mater. Sci., 28 (2005) 689.
28 G. W. Tomlins, J. L. Routbort and T. O. Mason, J. Appl. Phys., 87 (2000) 117.
29 P. Erhart and K. Albe, Phys. Rev. B, 73 (2006) 115207-1.
30 G. Vourlias, N. Pistofidis, D. Chaliambalias, K. Chrissafis, El. Pavlidou and G. Stergioudis, J. Therm. Anal. Cal., 87 (2007) 401.
31 G. Vourlias, N. Pistofidis, D. Chaliampalias, E. Pavlidou, G. Stergioudis, E. K. Polychroniadis and D. Tsipas, J. Alloys Compd., 416 (2006) 125.
32 G. Reumont, J. B. Vogt, A. Iost and J. Foct, Surf. Coat. Techol., 139 (2001) 265.
33 R. H. Unger, ASM Handbook, Vol. 5 – Surface Engineering, New York, ASM International, 2000.
34 PC Powder Diffraction Files, JCPDS-ICDD, 2000.

Received: November 27, 2006
Accepted: January 30, 2007
OnlineFirst: March 23, 2007

DOI: 10.1007/s10973-006-8280-0